

periments of Kerns and Johnson⁸ in which observations were made of a 2.5-MV, 25-kA stream formed from a Bennett cathode and incident on a $(\text{CD}_2)_n$ target. It was found that ~ 21 kA of stream current was focused to a diameter $\lesssim 75 \mu\text{m}$ in a time ~ 25 nsec following filamentation at ~ 15 nsec. Filamentation and pinching initiated in the high-density plasma plume in front of the target. Typical values were $\gamma \approx 6$, $i \approx 0.2$, $Z \approx \frac{8}{3}$, $\sigma_0 \approx 0.1$ cm, and $\sigma \approx 3.75 \times 10^{-3}$ cm. Then, by calculation $f \approx 35$, $\psi \approx 0.58$ (i.e., ~ 300 keV), $\lambda \approx 0.224$ cm, $\sigma_f \approx 0.54 \times 10^{22} n^{-1}$ cm, $L \approx 2.4 \times 10^{22} n^{-1}$ cm, $t_d \approx 18.8$ nsec, with the requirement that $n > 3.6 \times 10^{16} \text{ cm}^{-3}$. The time equivalent to t_i (i.e., the time taken for formation of a dense plasma within the stream) is determined, in this case, by closure of the 0.6-cm cathode-anode gap by plasma plumes from the cathode and anode surfaces.⁹ The observed times⁸ were consistent with established plasma-diode dynamics.⁹ For all expected ranges of n in the diode, σ_f and L greatly exceeded experimental dimensions. Thus, $\sigma_0 \ll \sigma_f$ and uniform-diameter conditions should exist after the 0.224-cm focusing distance. Then from Eq. (9), $\psi_0 \approx \gamma i (\beta \sigma / \sigma_0)^2 / 2 \approx 0.84 \times 10^{-3}$ (corresponding to ≈ 430 eV) is necessary in order to achieve the observed pinch radius. Such values, attainable with the Bennett cathode, are thought to occur due to channeling of cathode-emission electrons to the diameter of the dielectric rod before these particles have gained appreciable energy from the applied field. Such behavior would not occur, for example, in large-aspect-ratio diodes where stream electrons acquire appreciable energies before focusing occurs.

Of interest here is the behavior of the stream

as it penetrates the solid target. Taking as initial conditions the values $\sigma_0 \approx 3.75 \times 10^{-3}$ cm and $\psi_0 \approx 0.58$ attained within the diode, the solid-density parameters $n \approx 10^{23} \text{ cm}^{-3}$ and $Z \approx \frac{8}{3}$ give $\sigma_f \approx 0.054 \text{ cm} \gg \sigma_0$, $\sigma \approx \sigma_0 \approx 3.75 \times 10^{-3}$ cm, $\psi \approx \psi_0 \approx 0.58$, $\lambda \approx 8.4 \times 10^{-3}$ cm, $L \approx 0.242$ cm, $t_i(+1) \approx 0.32$ nsec, and $t_d \approx 0.7$ nsec. Thereby, it appears that very rapidly the stream penetrates the solid over distances of several millimeters at a uniform diameter $\lesssim 75 \mu\text{m}$. Under such conditions, power flux densities within the target may have exceeded $1.6 \times 10^{15} \text{ W/cm}^2$ in these experiments.

These considerations were aided by discussions with J. J. Wynne.

¹D. L. Morrow, J. D. Phillips, R. M. Stringfield, Jr., W. O. Doggett, and W. H. Bennett, *Appl. Phys. Lett.* **19**, 441 (1971).

²H. Alfvén, *Phys. Rev.* **55**, 425 (1939).

³R. A. McCorkle, *Phys. Rev. A* **11**, 2152 (1975).

⁴M. Inokuti, *Rev. Mod. Phys.* **43**, 297 (1971); F. F. Rieke and W. Prepejchal, *Phys. Rev. A* **6**, 1507 (1972); A. Salop, *Phys. Rev. A* **9**, 2496 (1974); A. Crispin and E. N. Fowler, *Rev. Mod. Phys.* **42**, 290 (1970).

⁵R. Lee and R. N. Sudan, *Phys. Fluids* **14**, 1213 (1971); A. A. Rukhadze and V. G. Rukhlin, *Zh. Eksp. Teor. Fiz.* **61**, 177 (1971) [*Sov. Phys. JETP* **34**, 93 (1972)].

⁶R. A. McCorkle, *J. Phys. A: Math. Gen.* **8**, 987 (1975).

⁷L. H. Thomas, *Proc. Roy. Soc., London* **121**, 464 (1928).

⁸J. R. Kerns and D. J. Johnson, *J. Appl. Phys.* **45**, 5225 (1974).

⁹L. P. Mix, J. G. Kelly, G. W. Kuswa, D. W. Swain, and J. N. Olsen, *J. Vac. Sci. Technol.* **10**, 951 (1973).

Plasma Resonance in the X-Ray Emission from Gaseous Laser Targets

Eli Yablonovitch

Gordon McKay Laboratory, Harvard University, Cambridge, Massachusetts 02138

(Received 18 August 1975)

I report the first observation of CO_2 -laser-induced x-ray emission from *gaseous* targets. By varying the gas pressure, the plasma density of the target was tuned through resonance at the critical density. The x-ray emission rose quickly from zero at the critical pressure, and reached a peak when the plasma was slightly overdense. Because of the resonant enhancement, a CO_2 -laser pulse of only 0.1 J was sufficient for this experiment.

In the interaction between a laser pulse and a solid target, the plasma density varies from $\sim 10^{23}$ electrons/cm³ in the target to 0 in the sur-

rounding vacuum. It is generally agreed¹ that the energy absorption takes place in the narrow critical layer where the plasma frequency equals the

laser frequency ω . Nevertheless, there is no consensus on the absorption mechanism itself. Some theorists favor a type of nonlinear parametric interaction,² while others invoke a linear resonance model.³

In order to elucidate the physics of the resonant interaction process itself, it is desirable to control the plasma density to be at or near the critical density. In studying the physics, therefore, a gaseous target may be more appropriate than a solid target. For example, when hydrogen gas at 150 Torr becomes fully ionized, the plasma density is $10^{19}/\text{cm}^3$, the critical density for the CO_2 -laser frequency. Thus by varying the gas pressure in the neighborhood of 150 Torr we can study the underdense regime, the resonant regime, and the overdense regime. Similarly for any other gas, there will be a critical pressure which depends on the charge state of the positive ions which are formed.

In this paper I report x-ray emission from plasmas produced in hydrogen, helium, mixtures of hydrogen and helium, nitrogen, argon, and helium doped with 1% xenon.

The laser source was a CO_2 oscillator, followed by an optical free-induction-decay pulse shaper,⁴ with a Lumonics 103 used as a final-stage amplifier. This system is more fully described by Kwok and Yablonovitch.⁵ The output is a diffraction-limited pulse of 0.1-J energy and 500-psec duration. It was focused into the gas cell with a spherically corrected, $f/1$; germanium, doublet lens. The gas was filtered and cold trapped to remove impurities which might cause premature breakdown.⁶ There was a steady flow through the chamber to ensure a fresh charge of gas for each laser shot.

The plasma was generated through avalanche ionization, driven by inverse-bremsstrahlung heating of the electrons. The focal-spot intensity was high enough to initiate⁷ the avalanche by tunneling.⁸ Below a certain pressure threshold, the gas would not break down, because of the reduction in collisional heating rate and the increase in diffusive loss rate of electrons.⁹ This varied from ~ 25 Torr in argon to about ~ 100 Torr in helium. Observations were made over a wide pressure range from the breakdown threshold up to 1 atm.

The resonant nature of the x-ray production is evident in Fig. 1 which plots it as a function of gas pressure. Hydrogen has the sharpest resonance. At the critical pressure of 150 Torr the emission rises from zero, quickly reaching a

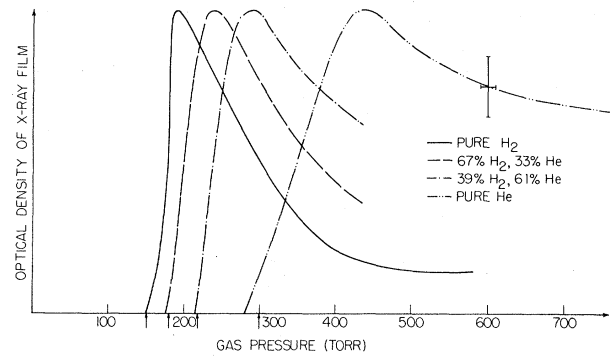


FIG. 1. X-ray emission from plasmas produced in hydrogen-helium mixtures. The four small arrows along the abscissa indicate the calculated gas pressure which would give rise to a critical density of electrons ($10^{19}/\text{cm}^3$) for each of the four mixtures, in order of decreasing hydrogen fraction. This shows that the onset of x-ray production occurs at the critical pressure. The emission is normalized to unity at the peak value.

maximum when the plasma is $\sim 25\%$ overdense. The x-ray production just below the critical pressure is under the limit of our detection capability, less than 2% of the peak emission. Helium has the same behavior except that the onset of x-ray emission is at 300 Torr, exactly twice the critical pressure of H_2 . This indicates that the helium plasma is produced in the singly ionized charge state, a result which will be explained later in the paper.

Particularly fascinating are the results on H_2 -He mixtures which show the shift of the resonance as a function of the concentration ratio. The small arrows along the abscissa give the calculated critical pressure, p_c , for each of the four mixtures in order of decreasing hydrogen fraction x :

$$p_c = kTm\omega^2/4\pi e^2(1+x),$$

where e and m are the charge and mass of the electron, T is room temperature, k is Boltzmann's constant, and ω is the laser frequency.

Helium gas doped with 1% xenon showed the same pressure dependence as pure He, but the emission was much stronger because of the high atomic number of xenon.

In Fig. 2 we see that argon and nitrogen also exhibit a form of resonant behavior. Because of the higher ionization state of which these gases are capable, the plasma resonance is shifted to lower pressures. We can infer a charge state of perhaps 4 or 5 for these atoms. The ambiguity

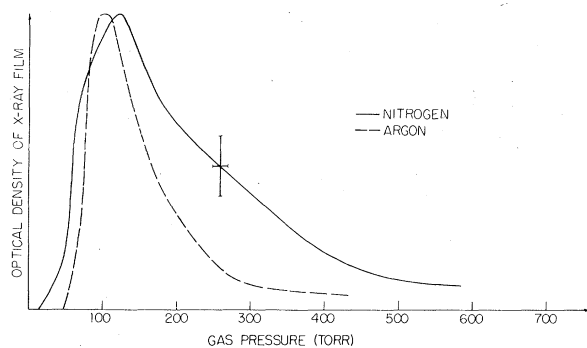


FIG. 2. X-ray emission from plasmas produced in nitrogen and argon. The emission is normalized to unity at the peak value.

in the precise degree of ionization is probably responsible for the smearing out of the resonance when compared to the sharp steplike behavior of a gas like hydrogen.

The radiation was detected by two means: (a) a silicon surface-barrier detector filtered by 6.9 mg/cm² of Al foil and placed about 1 cm from the focal region; (b) small film packets of Kodak no-screen medical x-ray film filtered by 10 mg/cm² of black polyethylene and placed about 0.8 cm from the focal region. Most of the quantitative measurements were made with the film, calibrations of which have recently been published.¹⁰

The experimental procedure was to expose the film for 20 min at a given gas pressure, with the laser pulsing at 0.3 pulses per second. The exposures had to be reduced for argon and for He:Xe, which, because of their higher atomic number, had much more powerful x-ray emission. Typically, the film was exposed to a net optical density of about 1.

The 10-mg/cm² polyethylene filter is essentially opaque to x-ray wavelengths longer than $\sim 8 \text{ \AA}$. Therefore only bremsstrahlung and free-bound continuum radiation could be observed from the low-*Z* gases (N₂, He, H₂), whose line emission is beyond the long wavelength cutoff of the filter. Employing the two-foil-absorber ratio technique, with foils of 10 and 20 mg/cm² of polyethylene, an effective electron temperature of 1 keV was inferred¹¹ for the nitrogen plasma.

There was an additional complication in the x-ray emission from H₂ and He. Because of their low atomic number, their bremsstrahlung and free-bound continuum radiation were very weak. Similarly, the stopping power of the gas for fast electrons was relatively small. Electrons were

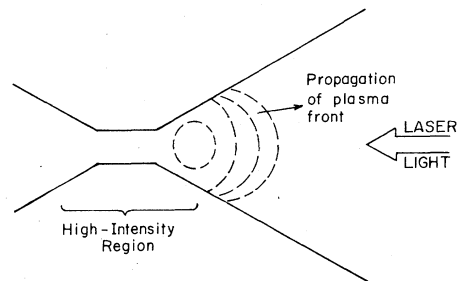


FIG. 3. The solid lines show the focal spot and the cone-shaped region of laser light leading to it. The dashed lines represent the ionization front at successive instants in time. Notice that the laser-plasma interaction occurs mainly in the low-intensity region in front of the focal spot.

emitted from the focal region with enough energy to strike a copper surface of the gas cell 8 mm away. Because of the relatively high *Z* of the metal, this roundabout mechanism produced x-rays comparable in intensity to the continuum coming directly from the focal region itself. In He the two contributions were about equal, while in H₂ the emission from the metal surface was the stronger of the two. From the range-energy relations¹² for the fast electrons, we can infer that at least 10 keV are required to penetrate 8 mm of gas and have enough energy left over to produce x rays. A study of the fast-electron emission will be published in a forthcoming paper.¹³

To interpret these experiments more fully, it is important to know the geometry of both the plasma and the light beam which is generating it. The optical electric field *E* is so high that the electron quiver energy $e^2 E^2 / 2m\omega^2$ greatly exceeds the ionization potential of the gas, not only in the focal spot, but also in the cone-shaped region of laser light leading to it, as shown in Fig. 3. Under these conditions, impact ionization occurs with every collision and is roughly independent of the light intensity. Since the diffusive loss rate of electrons from the tiny focal volume is quite high, the plasma will actually avalanche more quickly in the lower-intensity region in front of the focal spot where the beam width is larger. From there the ionization front will spread as a breakdown wave,¹⁴ further upstream toward the lens. In this relatively low-intensity region, the critical layer appears as a moving front, and this is where the resonant laser-plasma interaction actually occurs.

In the context of this picture, we can under-

stand why helium does not experience plasma resonance in the pressure range between 150 and 300 Torr, where a doubly ionized plasma would be resonant. Because of the factor 10 difference in ionization cross section¹⁵ and the factor 2 difference in ionization potential between He and He⁺, the avalanche ionization rate for the two species will be vastly different. Therefore a large cone-shaped region of singly ionized, slightly underdense, plasma will first form in front of the focal spot. This will defocus the light and prevent it from reaching a high intensity for a long enough time to produce the doubly ionized plasma. This reasoning does not apply to nitrogen and argon, because the difference in ionization cross section¹⁶ between successive stages of ionization is much less.

I would like to thank R. Godwin and G. H. McCall for many valuable discussions.

¹J. Nuckolls, L. Wood, A. Thiessen, and G. Zimmerman, *Nature* (London) **239**, 139 (1972).

²P. K. Kaw, J. Dawson, W. Krueer, C. Oberman, and E. Valeo, *Kvantovaya Elektron.* **1**, No. 3, 3 (1971) [*Sov. J. Quantum. Electron.* **1**, 205 (1971)]; M. N. Rosenbluth, R. B. White, and C. S. Liu, *Phys. Rev. Lett.* **31**, 1190 (1972).

³R. P. Godwin, *Phys. Rev. Lett.* **28**, 85 (1972); J. P. Friedberg, R. W. Mitchell, R. L. Morse, and L. I. Rudinsky, *Phys. Rev. Lett.* **28**, 795 (1972).

⁴E. Yablonovitch and J. Goldhar, *Appl. Phys. Lett.* **25**, 580 (1974).

⁵H. S. Kwok and E. Yablonovitch, *Rev. Sci. Instrum.* **46**, 814 (1975).

⁶E. Yablonovitch, *Phys. Rev. A* **10**, 1888 (1974).

⁷E. Yablonovitch, *Phys. Rev. Lett.* **31**, 877 (1973).

⁸L. V. Keldysh, *Zh. Eksp. Teor. Fiz.* **47**, 1945 (1964) [*Sov. Phys. JETP* **20**, 1307 (1965)].

⁹D. R. Cohn, C. E. Chase, W. Halverson, and B. Lax, *Appl. Phys. Lett.* **20**, 225 (1972); E. Yablonovitch, *Appl. Phys. Lett.* **23**, 122 (1973).

¹⁰See the articles by L. N. Koppel and R. A. Armistead, in *Advances in X-ray Analysis*, edited by W. L. Pickles, C. S. Barrett, J. B. Newkirk, and C. O. Rund (Plenum, New York, 1975), Vol. 18.

¹¹Based on data from R. C. Elton, NRL Technical Report No. 6541, 1967 (unpublished), and No. 6738, 1968 (unpublished).

¹²E. Segré, *Nuclei and Particles* (Benjamin, New York, 1965).

¹³E. Yablonovitch, to be published.

¹⁴Yu. P. Raizer, *Usp. Fiz. Nauk* **108**, 429 (1972) [*Sov. Phys. Usp.* **15**, 688 (1973)].

¹⁵H. S. W. Massey and E. H. S. Burhop, *Electronic and Ionic Impact Phenomena* (Oxford Univ. Press, London, 1969), Vol. 1.

¹⁶C. W. Allen, *Astrophysical Quantities* (Athlone Press, London, 1973).

Propagation of Ion-Acoustic Waves in a Two-Electron-Temperature Plasma*

W. D. Jones, A. Lee, S. M. Gleman, and H. J. Doucet†

Department of Physics, University of South Florida, Tampa, Florida 33620

(Received 25 August 1975)

The propagation of ion-acoustic waves (IAW) in a double-electron-temperature plasma is investigated both experimentally and theoretically. It is found that the presence of even a small fraction of the lower-electron-temperature component can dominate the behavior of the waves. The results have important implications both for the use of IAW as a diagnostic tool for measuring electron temperature and for the interpretation of turbulent IAW spectra.

In this paper, we examine the propagation of linear ion-acoustic waves (IAW) in a plasma whose electron velocity distribution may be represented by the superposition of two Maxwellians.¹ Such electron distributions are rather frequently encountered. For example, hot turbulent plasmas of thermonuclear interest often have high-energy tails; strong electron-beam-plasma interactions can result in such electron distributions; and very often, simple hot-cathode discharge plasmas also have double-electron-tem-

perature distributions.^{1,2} The latter type of plasma is used in the present study because it is steady state, quiescent, and the plasma parameters are easily varied over a fairly wide range.

When two groups of electrons at different temperatures are present, the Langmuir-probe current characteristic shows a distinct break in the electron-retardation region. An example is given in Fig. 1. The procedure for determining both the temperatures and the densities of the two electron distributions is well known.¹